Integrity Analysis of Cascaded Integer Resolution with Decorrelation Transformations

P. Henkel[†] and C. Günther[†,‡]
[†]*Technische Universität München (TUM), Germany*
[‡]*Deutsches Zentrum für Luft- und Raumfahrt (DLR), Germany*

BIOGRAPHIES

Patrick Henkel has studied Electrical Engineering and Information Technology at the Technische Universität München (TUM), Germany and the École Polytechnique de Montréal, Canada. He is now a PhD student at the Institute of Communications and Navigation of TUM. His research interests focus on the integrity of carrier phase measurements.

Christoph Günther studied theoretical physics at the Swiss Federal Institute of Technology in Zurich. He received his diploma in 1979 and completed his PhD in 1984. He worked on communication and information theory at Brown Boveri and Ascom Tech. From 1995, he led the development of mobile phones for GSM and later dual mode GSM/Satellite phones at Ascom. In 1999, he became head of the research department of Ericsson in Nuremberg. Since 2003, he is the director of the Institute of Communication and Navigation at the German Aerospace Center (DLR) and since December 2004, he additionally holds a Chair at the Technische Universität München (TUM). His research interests are in satellite navigation, communication, and signal processing.

ABSTRACT

A method for the resolution of the integer ambiguities of double difference carrier phase measurements is studied with respect to its integrity.

The method is an enhancement of the Three-Carrier Ambiguity Resolution (TCAR) method introduced by Forssell, Neira and Harris in [1] and the Cascade Integer Resolution (CIR) considered by Jung, Enge and Pervan. The proposed method is based on a full-geometry approach, i.e. the code and phase measurements of all satellites are considered as a set. Decorrelation and rounding steps of the LAMBDA method are performed successively on the Galileo Super Wide Lane (SWL) and Widelane (WL) carrier combinations and the E5a carrier. The probability of wrong fixing for the WL combination L1-E5a is greatly reduced by the a-priori knowledge of the SWL ambiguity. An optimized choice of WL combination $(-4.121\phi_{\mathrm{L1}}+39.831\phi_{\mathrm{E5b}}-34.800\phi_{\mathrm{E5a}})$ further improves the result by several orders of magnitude without much affecting the ionospheric delay. The probability distribution of the baseline error is estimated using an importance sampling approach. This probability distribution leads to a Galileo like implicit definition of Horizontal and Vertical Protection Levels (XPL) for carrier phase measurements. The new definition can be used to detect a wrong fixing at one level, e.g. X=WL, whenever the protection level at the previous level, SWL in the current example, is smaller than the smallest baseline error due to a wrong fixing at the X level.

INTRODUCTION

Carrier phase based positioning requires the resolution of integer ambiguities. The Least-Squares Ambiguity Decorrelation Adjustment (LAMBDA) has been developed by Teunissen in [2][3]. Implementation aspects are described by Jonge and Tiberius in [4]. The method is especially beneficial for correlated double difference measurements with a common reference satellite. An integer decorrelation transformation is applied before the search of integer ambiguities. The LAMBDA method achieves the highest success rates among all methods known to the authors. Cascade Integer Resolution (CIR) is an iterative approach where the integer ambiguities of widelane combinations with successively reduced wavelengths are estimated. The range and ionospheric delay as well as ambiguities are commonly estimated using three GPS frequencies by Jung et al. in [5]. Each range is resolved individually, i.e. satellite redundancy is not taken into account.

A systematic search of all GPS L1-L2 widelane combinations has been performed by Collins in [6] and the references therein. The linear combinations are characterized by noise, ionosphere and multipath amplification/ reduction. For Galileo, three frequency combinations have been analysed by Zhang in [7] although the wavelengths of the considered three frequency combinations do not exceed 90 cm. The LAMBDA method is applied to each step of CIR but the benefits of the various steps of LAMBDA are not compared. The optimization of linear combinations in [7] is based on noise figures and does not include the decorrelation transformation.

The paper is structured as follows. First, the LAMBDA algorithm is introduced for Galileo widelane combinations. Three steps of CIR are considered - the E5a-E5b Super Widelane (SWL), the L1-E5a Widelane (WL) and the elementary L1, E5b and E5a measurements. In the first CIR step, the code noise variance has a large impact on the success rate although the decorrelation transformation might additionally reduce the probability of wrong rounding by up to three orders of magnitude. The benefit of SWL a priori knowledge, decorrelation transformations, search processes and code knowledge are compared in the second step. The third step is the most reliable one due to a priori knowledge of both SWL and WL integer ambiguities.

In the next section, the WL combination is optimized for CIR such that the success rate is maximized for worst-case geometry and a priori SWL knowledge. It is shown that the probability of wrong WL fixing can be reduced by 15 orders of magnitude. The success rate using the optimized WL combination is nearly independent of the geometry, i.e. the price of lower error probabilities for bad geometry is an increase in error rates for good geometry.

Moreover, the probability distribution of the error of baseline estimation is derived. A mixed multivariate probability distribution is assumed to include error-prone ambiguity fixing. The probabilities of most likely fixing errors are computed by importance sampling. The decorrelation transformations are taken into account.

Protection levels are implicitly defined by the probability distribution of the error of baseline estimation. Finally, the SWL protection levels are applied for detection and exclusion of WL biases due to error-prone WL fixing.

APPLICATION OF DECORRELATION TRANSFORMATIONS TO WIDELANE COMBINATIONS

Double Difference (DD) measurements eliminate clock biases and reduce both ionospheric and tropospheric errors especially for short baselines. Phase measurements from two frequencies are differenced to obtain a Widelane (WL) combination. This widelane signal benefits from a wavelength larger than the elementary ones which simplifies integer ambiguity resolution. However, the use of difference measurements also implies noise amplification. Cascade Integer Resolution (CIR) [5] is an iterative approach for ambiguity resolution with widelane combinations of successively reduced wavelengths.

The first step refers to the E5a-E5b SWL combination which can be decomposed into

$$\begin{bmatrix} \lambda_{\mathrm{SWL}} \cdot \boldsymbol{\phi}_{\mathrm{SWL}} \\ \boldsymbol{\rho} \end{bmatrix} = \begin{bmatrix} \boldsymbol{G} \\ \boldsymbol{G} \end{bmatrix} \boldsymbol{\delta x} + \begin{bmatrix} \mathbf{1} \\ \mathbf{0} \end{bmatrix} \cdot \lambda_{\mathrm{SWL}} \boldsymbol{N}_{\mathrm{SWL}} + \begin{bmatrix} \boldsymbol{\varepsilon}_{\mathrm{SWL}} \\ \boldsymbol{\varepsilon}_{\rho} \end{bmatrix}, \quad (1)$$

with the wavelength $\lambda_{\mathrm{SWL}} = 9.76\mathrm{m}$, the SWL DD phase measurements $\boldsymbol{\phi}_{\mathrm{SWL}}$, the DD code measurements $\boldsymbol{\rho}$, the DD geometry matrix $\boldsymbol{G}$ and the DD phase/ code noise $\boldsymbol{\varepsilon}_{\mathrm{SWL}}, \boldsymbol{\varepsilon}_{\rho}$. The baseline $\boldsymbol{\delta x}$ and the SWL DD integer ambiguities $\boldsymbol{N}_{\mathrm{SWL}}$ are the parameters to be estimated.

In the second step, the L1-E5a WL combination ($\lambda_{\mathrm{WL}} = 0.75\mathrm{m}$) is considered. In contrast to traditional approaches, both the SWL and code measurements with the a priori known SWL ambiguities are taken into account:

$$\begin{bmatrix} \lambda_{\mathrm{SWL}} \cdot (\boldsymbol{\phi}_{\mathrm{SWL}} - \boldsymbol{N}_{\mathrm{SWL}}) \\ \lambda_{\mathrm{WL}} \cdot \boldsymbol{\phi}_{\mathrm{WL}} \\ \boldsymbol{\rho} \end{bmatrix} = \begin{bmatrix} \boldsymbol{G} \\ \boldsymbol{G} \\ \boldsymbol{G} \end{bmatrix} \boldsymbol{\delta x} + \begin{bmatrix} \mathbf{0} \\ \mathbf{1} \\ \mathbf{0} \end{bmatrix} \cdot \lambda_{\mathrm{WL}} \boldsymbol{N}_{\mathrm{WL}} + \begin{bmatrix} \boldsymbol{\varepsilon}_{\mathrm{SWL}} \\ \boldsymbol{\varepsilon}_{\mathrm{WL}} \\ \boldsymbol{\varepsilon}_{\rho} \end{bmatrix}. \quad (2)$$

In the final step, the E5a, E5b and L1 DD phase and code measurements are used for fixing the E5a integer ambiguities, i.e.

$$\begin{bmatrix} \lambda_{\mathrm{E5a}} \cdot (\boldsymbol{\phi}_{\mathrm{E5a}}) \\ \lambda_{\mathrm{E5b}} \cdot (\boldsymbol{\phi}_{\mathrm{E5b}} - \boldsymbol{N}_{\mathrm{SWL}}) \\ \lambda_{\mathrm{L1}} \cdot (\boldsymbol{\phi}_{\mathrm{L1}} - \boldsymbol{N}_{\mathrm{WL}}) \\ \boldsymbol{\rho} \end{bmatrix} = \begin{bmatrix} \boldsymbol{G} \\ \boldsymbol{G} \\ \boldsymbol{G} \\ \boldsymbol{G} \end{bmatrix} \boldsymbol{\delta x} + \begin{bmatrix} \lambda_{\mathrm{E5a}} \cdot \mathbf{1} \\ \lambda_{\mathrm{E5b}} \cdot \mathbf{1} \\ \lambda_{\mathrm{L1}} \cdot \mathbf{1} \\ \mathbf{0} \end{bmatrix} \cdot \boldsymbol{N}_{\mathrm{E5a}} + \begin{bmatrix} \boldsymbol{\varepsilon}_{\mathrm{E5a}} \\ \boldsymbol{\varepsilon}_{\mathrm{E5b}} \\ \boldsymbol{\varepsilon}_{\mathrm{L1}} \\ \boldsymbol{\varepsilon}_{\rho} \end{bmatrix}. \quad (3)$$

Note that the L1 and E5b integer ambiguities can be expressed as a function of the E5a, WL and SWL integer ambiguities. The model of the covariance matrix includes both the correlation due to DD with a common reference station/ reference satellite and the correlation due to the SWL and WL dependency on E5a measurements. The covariance matrix is given by

$$\boldsymbol{\Sigma} = \begin{bmatrix} \boldsymbol{\Sigma}_{\phi} & \mathbf{0} \\ \mathbf{0} & \boldsymbol{\Sigma}_{\rho} \end{bmatrix} \otimes \begin{bmatrix} 4 & 2 & 2 & \cdots \\ 2 & 4 & 2 & \\ 2 & 2 & 4 & \\ \vdots & & & \end{bmatrix}, \quad (4)$$

where $\otimes$ denotes the Kronecker product [11]. The inter-frequency correlation covariance matrix $\boldsymbol{\Sigma}_{\phi}$ of phase measurements of Equation (2) can be written as

$$\boldsymbol{\Sigma}_{\phi} = \sigma_{\phi}^{2} \cdot \begin{bmatrix} \left(\frac{\lambda_{\mathrm{SWL}}}{\lambda_{\mathrm{E5a}}}\right)^2 + \left(\frac{\lambda_{\mathrm{SWL}}}{\lambda_{\mathrm{E5b}}}\right)^2 & \frac{\lambda_{\mathrm{WL}} \cdot \lambda_{\mathrm{SWL}}}{\lambda_{\mathrm{E5a}}^2} \\ \frac{\lambda_{\mathrm{WL}} \cdot \lambda_{\mathrm{SWL}}}{\lambda_{\mathrm{E5a}}^2} & \left(\frac{\lambda_{\mathrm{WL}}}{\lambda_{\mathrm{L1}}}\right)^2 + \left(\frac{\lambda_{\mathrm{WL}}}{\lambda_{\mathrm{E5a}}}\right)^2 \end{bmatrix}. \quad (5)$$

No WL combinations are applied to code measurements, i.e. the code covariance is assumed $\boldsymbol{\Sigma}_{\rho} = \sigma_{\rho}^2 \mathbf{1}$. The twofold correlation of WL DD carrier phase measurements motivates the use of a decorrelation transformation. The LAMBDA algorithm of Teunissen [2] first estimates the float solution $(\boldsymbol{\delta}\hat{\boldsymbol{x}}, \hat{\boldsymbol{N}})$ neglecting the integer nature of ambiguities. A decorrelation transformation is applied to the float ambiguities before a search process is investigated in the transformed space. Finally, the fixed integer ambiguities are transformed back into the original domain. The design of the decorrelation transformation $\boldsymbol{Z}$ is constrained by the requirement that both $\boldsymbol{Z}$ and it's inverse are integer valued. The second constraint is fulfilled if $\det(\boldsymbol{Z}) = 1$. The decorrelation transformation $\boldsymbol{Z}$ depends only on the covariance matrix of float ambiguities and is computed by alternating steps of integer approximated Gaussian eliminations and ambiguity permutations [4]. The transformed ambiguities are largely decorrelated and also benefit from a reduced variance. In the following analysis, the search process $\mathcal{S}$ includes the estimation of the search space volume [3].

For simplicity, the combined phase and code measurements of Equation (1), (2) or (3) are rewritten as

$$\boldsymbol{y} = \boldsymbol{G}\boldsymbol{\delta x} + \boldsymbol{A}\boldsymbol{N} + \boldsymbol{\varepsilon} = \underbrace{[\boldsymbol{A}, \boldsymbol{G}]}_{\boldsymbol{X}} \underbrace{\begin{bmatrix} \boldsymbol{N} \\ \boldsymbol{\delta x} \end{bmatrix}}_{\boldsymbol{\beta}} + \boldsymbol{\varepsilon}, \quad (6)$$

with the least-squares float solution

$$\hat{\boldsymbol{\beta}} = (\boldsymbol{X}^T \boldsymbol{\Sigma}^{-1} \boldsymbol{X})^{-1} \boldsymbol{X}^T \boldsymbol{\Sigma}^{-1} \boldsymbol{y}. \quad (7)$$

The LAMBDA based estimate of integer ambiguities is given by

$$\check{\boldsymbol{N}} = (\boldsymbol{Z}^T)^{-1} \mathcal{S}\left(\hat{\mathrm{N}}'\right) = (\boldsymbol{Z}^T)^{-1} \mathcal{S}\left(\boldsymbol{Z}^T \boldsymbol{T} \hat{\boldsymbol{\beta}}\right), \quad (8)$$

with the ambiguity selection matrix $\boldsymbol{T} = [\mathbf{1}, \mathbf{0}]$ and the search function $\mathcal{S}$. The covariance matrix of decorrelated float ambiguities is given by

$$\boldsymbol{\Sigma}_{\hat{N}'} = \boldsymbol{Z}^T \boldsymbol{T} \left(\boldsymbol{X}^T \boldsymbol{\Sigma}^{-1} \boldsymbol{X}\right)^{-1} \boldsymbol{T}^T \boldsymbol{Z}. \quad (9)$$

The most simple model of the search process is the rounding of decorrelated ambiguities. The probability of wrong rounding is given by Verhagen in [9]:

$$P_{\mathrm{w}} = 1 - \prod_{i=1}^{N_{\mathrm{s}}-1} \int_{-0.5}^{+0.5} p_i(x) dx, \quad (10)$$

where N_{s} denotes the number of visible satellites. The remaining correlation has been neglected and $p_i(x) \sim \mathcal{N}\left(0, \boldsymbol{\Sigma}_{\hat{N}'}(i,i)\right)$. In contrast to the decorrelation transformation, the search process depends itself on the float ambiguities. The analysis of the benefit of the search process over simple rounding requires the generation of measurement samples. For low error probabilities, this might become intractable.

A three frequency Galileo receiver (L1, E5b, E5a) with $5°$ elevation mask and 10 km baseline is modeled. The reference station is located in southern Bavaria ($48°$ N,$11°$ E). The analysis restricts to single epoch measurements for real-time ambiguity resolution.

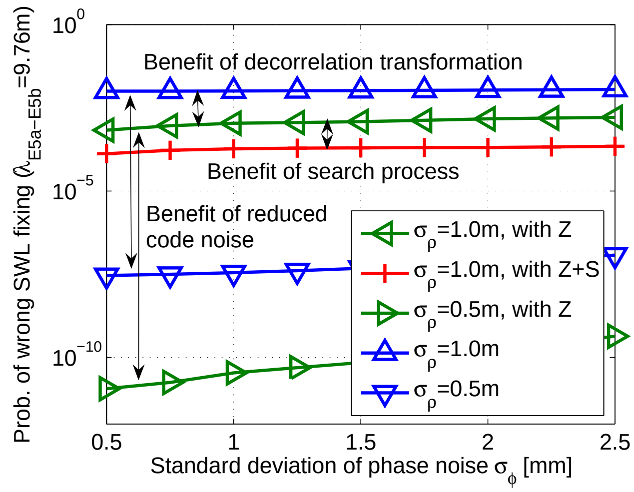

Fig. 1 First step of CIR: Fixing of SWL ambiguities for worst-case geometry and variable code noise

Fig. 1 shows the probability of wrong SWL fixing as a function of the phase noise. The benefit of both decorrelation transformation and search process and the impact of code noise variance on the success rate can be observed. The code noise limits the success rate, i.e. σ_ρ has a far higher impact on the success rate than σ_ϕ. For $\sigma_\rho = 0.5$ m, the decorrelation transformation reduces the probability of wrong rounding by up to three orders of magnitude.

The probability of wrong WL fixing for worst-case geometry is visualized in Fig. 2. The benefit of the SWL a priori knowledge exceeds the benefit of the decorrelation transformation and the search process. The usefulness of decorrelation/ search increases with lower phase noise variance and amounts to four orders of magnitude for $\sigma_\phi = 1$ mm. In contrast to the first CIR step, the success rate strongly depends on the phase noise variance but is rather insensitive w.r.t. the code noise variance.

Fig. 3 shows the probability of wrong E5a ambiguity fixing for variable phase noise variance. Obviously, the WL a priori knowledge has a larger benefit than the SWL a priori knowledge. The decorrelation transformation is twice as useful as the SWL measurements. Comparing the three steps of CIR, the conditional probabilities of Fig. 3 are lower than of the previous steps.

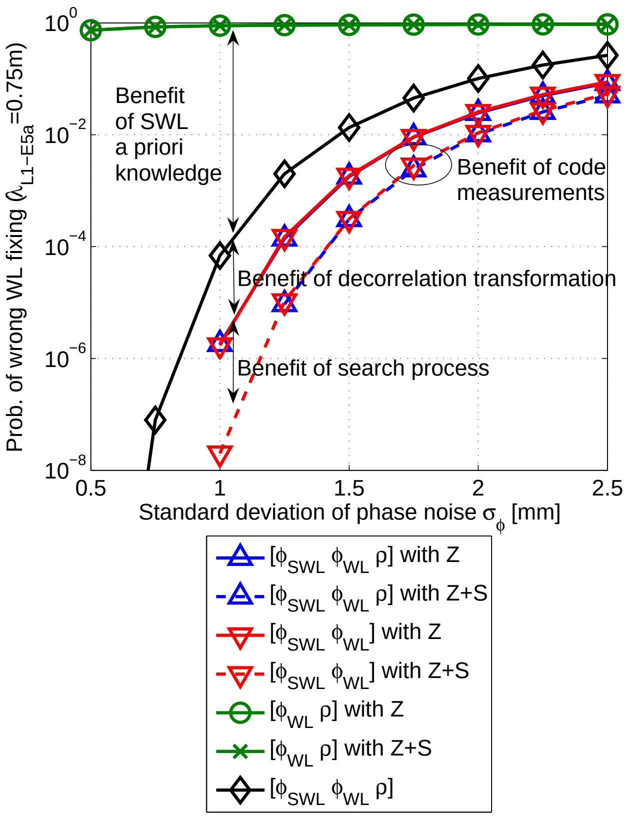

Fig. 2 Second step of CIR: Fixing of WL ambiguities for worst-case geometry and code noise $\sigma_\rho = 1\mathrm{m}$

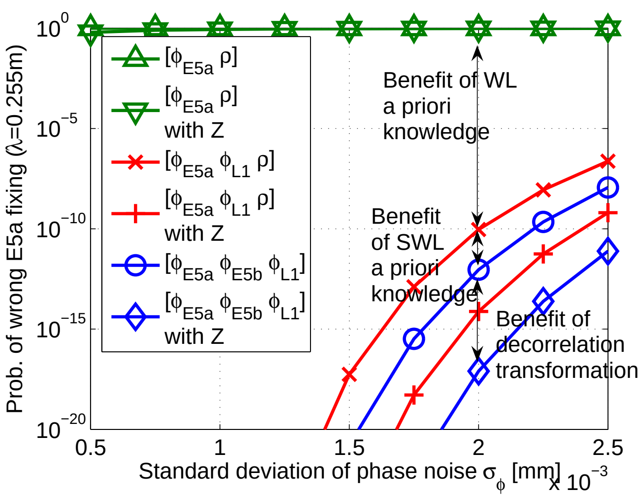

Fig. 3 Third step of CIR: Fixing of E5a ambiguities for worst-case geometry and code noise $\sigma_\rho = 1\mathrm{m}$

OPTIMIZATION OF WIDELANE COMBINATION FOR CASCADE INTEGER RESOLUTION

The (unit) widelane combination L1-E5a is not the only possible one. A systematic search for all possible L1-L2 GPS widelanes has been been performed by Collins in [6]. The concept was extended to the 3 Galileo frequencies (L1, E5b and E5a) by Zhang in [7]. The DD measurements are linearly combined by weighting coefficients α, β and γ:

$$\begin{aligned} \lambda\phi &= \alpha\lambda_1\phi_1 + \beta\lambda_2\phi_2 + \gamma\lambda_3\phi_3 \\ &= \rho(\alpha+\beta+\gamma) + (\alpha\lambda_1 N_1 + \beta\lambda_2 N_2 + \gamma\lambda_3 N_3) \\ &\quad -I_1(\alpha + \beta q_{12}^2 + \gamma q_{13}^2) + T(\alpha+\beta+\gamma) + \varepsilon, \end{aligned} \tag{11}$$

where λ denotes the wavelength of the Linear Combination (LC), ρ the DD range, I_1 the DD ionospheric delay on L1, T the DD tropospheric delay and q_{ij} the ratio between frequency f_i and f_j. The ionospheric delay is addressed in the present section, since the amplification of the ionospheric delay by the combination process must also be considered. Two restrictions are imposed to the design of weighting coefficients: First, the geometry part of the linear combination should be maintained, i.e.

$$\alpha + \beta + \gamma = 1. \tag{12}$$

Secondly, the ambiguity of the widelane combination should be an integer multiple N of a single wavelength λ:

$$\alpha\lambda_1 N_1 + \beta\lambda_2 N_2 + \gamma\lambda_3 N_3 = \lambda N. \tag{13}$$

This requirement is fulfilled by the following choice:

$$\frac{\alpha\lambda_1}{\lambda} \stackrel{!}{=} i, \ \frac{\beta\lambda_2}{\lambda} \stackrel{!}{=} j, \ \frac{\gamma\lambda_3}{\lambda} \stackrel{!}{=} k, \tag{14}$$

with the integer coefficients i, j and k. Once these integer weights are fixed, Equation (14) determines the weighting coefficients α, β and γ. The wavelength of the linear combination is obtained from Equations (12) and (14) as

$$\lambda = \frac{1}{\frac{i}{\lambda_1} + \frac{j}{\lambda_2} + \frac{k}{\lambda_3}} = \frac{\lambda_1\lambda_2\lambda_3}{i\lambda_2\lambda_3 + j\lambda_1\lambda_3 + k\lambda_1\lambda_2}. \tag{15}$$

Assuming $\lambda_1 < \lambda_2 < \lambda_3$, the WL criterion ($\lambda > \lambda_3$) for any set (i, j, k) is given by

$$\lambda_1\lambda_2 > i\lambda_2\lambda_3 + j\lambda_1\lambda_3 + k\lambda_1\lambda_2 > 0. \tag{16}$$

For a given pair (i, j), the third parameter is fixed by this inequality and given by

$$k = \lceil -(iq_{13} + jq_{23}) \rceil. \tag{17}$$

Replacing k in Equation (15) yields:

$$\lambda(i,j) = \frac{\lambda_3}{iq_{13} + jq_{23} + \lceil -(iq_{13} + jq_{23}) \rceil}. \tag{18}$$

Linear independent combinations require an additional constraint:

$$\gcd(i,j,k) \stackrel{!}{=} 1, \tag{19}$$

where $\gcd(\cdot)$ denotes the greatest common divisor.

The WL combination of the second CIR step is selected among all linear combinations such that the probability of wrong rounding (Equation 10) of decorrelated ambiguities is minimized. The optimization refers to the system of Equations in (2) and worst-case geometry. The covariance matrix in Equation (5) is adapted to include the correlation between SWL and LC measurements. Tab. 1 shows the obtained LCs of lowest probability of wrong rounding. The depicted combinations are characterized by equal success rates and are sorted according to the amplification $A_{\mathrm{I}} = |\alpha + \beta q_{12}^2 + \gamma q_{13}^2|$ of the DD ionospheric delay.

i	j	k	λ	A_{I}
-3	38	-34	0.2617	1.46
-3	37	-33	0.2689	1.54
-3	36	-32	0.2765	1.64
-3	35	-31	0.2845	1.74
-3	34	-30	0.2931	1.84
-3	33	-29	0.3021	1.95
-3	32	-28	0.3118	2.07

Table 1 Integer ambiguity coefficients of selected L1, E5b and E5a linear combinations with wavelength λ

In Fig. 4, the probability of wrong fixing is compared between the L1-E5a WL and the optimized LC. The proper choice of LCs enables a reduction of this probability by 15 orders of magnitude. Moreover, the optimized LC benefits from a three times lower wavelength ($\lambda_{\mathrm{LC}} \approx 26.1\mathrm{cm}$) than the unit WL. Note that the amplification of DD ionospheric delays might slightly reduce the achievable gain of optimized LC.

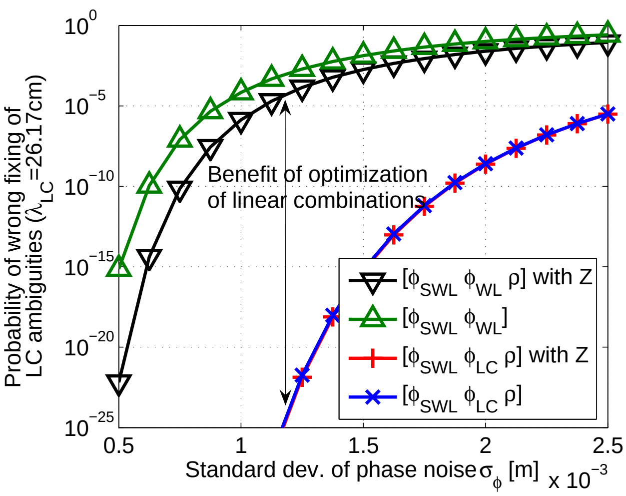

Fig. 4 Optimization of linear widelane combinations for 2nd step of CIR: Weighting $[-3, 38, -34]$ of L_1, $E_{5\mathrm{b}}$ and $E_{5\mathrm{a}}$ integer ambiguities

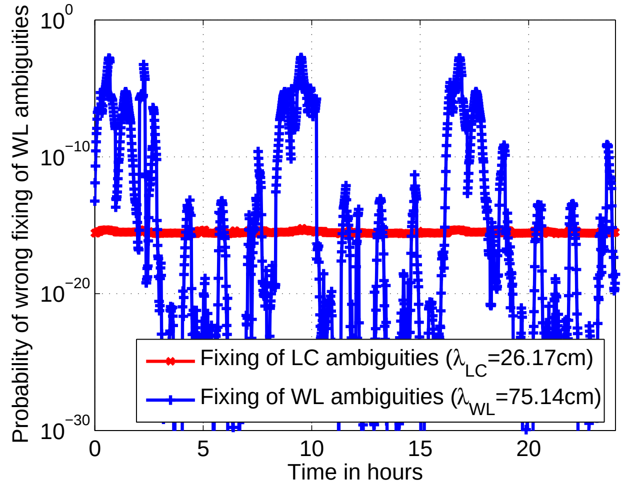

Fig. 5 Second step of CIR: Time dependency of probability of wrong fixing for different widelane combinations

The temporal dependency of the probability of wrong WL fixing with a priori SWL knowledge is shown in Fig. 5. The standard deviations of phase and code noise are assumed to be $\sigma_\phi = 1.5\mathrm{mm}$ and $\sigma_\rho = 1\mathrm{m}$.

The success rate for fixing LC ambiguities is rather insensitive w.r.t geometry (Fig. 5) in contrast to the unit L1-E5a WL ambiguities. Consequently, the critical peaks in the probability of wrong fixing could be eliminated and the maximum probability of wrong fixing is lowered from $1.8 \cdot 10^{-3}$ to $6.0 \cdot 10^{-16}$. The price is an increase in the probability of wrong fixing for good geometry.

ESTIMATION OF PROBABILITY DISTRIBUTION OF BASELINE ERROR

An integer estimate of rounded decorrelated ambiguities after back-transformation is given by Equations (8) and (7):

$$\begin{aligned} \check{N} &= (\boldsymbol{Z}^T)^{-1}\mathcal{S}\left(\boldsymbol{Z}^T\boldsymbol{T}(\boldsymbol{X}^T\boldsymbol{\Sigma}^{-1}\boldsymbol{X})^{-1}\boldsymbol{X}^T\boldsymbol{\Sigma}^{-1}\boldsymbol{y}\right) \\ &= (\boldsymbol{Z}^T)^{-1}\left[\boldsymbol{Z}^T\boldsymbol{T}(\boldsymbol{X}^T\boldsymbol{\Sigma}^{-1}\boldsymbol{X})^{-1}\right. \\ &\quad \left.\boldsymbol{X}^T\boldsymbol{\Sigma}^{-1}(\boldsymbol{A}\boldsymbol{N} + \boldsymbol{G}\boldsymbol{\delta x} + \boldsymbol{\varepsilon})\right], \end{aligned} \tag{20}$$

which can be simplified using the matrix properties

$$\begin{aligned} (\boldsymbol{X}^T\boldsymbol{\Sigma}^{-1}\boldsymbol{X})^{-1}\boldsymbol{X}^T\boldsymbol{\Sigma}^{-1}\boldsymbol{A} &= \begin{bmatrix} \mathbf{1}^{N_{\mathrm{s}}-1\times N_{\mathrm{s}}-1} \\ \mathbf{0}^{3\times N_{\mathrm{s}}-1} \end{bmatrix} \\ (\boldsymbol{X}^T\boldsymbol{\Sigma}^{-1}\boldsymbol{X})^{-1}\boldsymbol{X}^T\boldsymbol{\Sigma}^{-1}\boldsymbol{G} &= \begin{bmatrix} \mathbf{0}^{N_{\mathrm{s}}-1\times 3} \\ \mathbf{1}^{3\times 3} \end{bmatrix}, \end{aligned} \tag{21}$$

where N_{s} denotes the number of visible satellites. Integer terms are not affected by the rounding $[\cdot]$ and can be separated, i.e.

$$\begin{aligned}\check{\boldsymbol{N}} &= (\boldsymbol{Z}^T)^{-1}\left[\boldsymbol{Z}^T\boldsymbol{N}+\boldsymbol{Z}^T\boldsymbol{T}(\boldsymbol{X}\boldsymbol{\Sigma}^{-1}\boldsymbol{X})^{-1}\boldsymbol{X}^T\boldsymbol{\Sigma}^{-1}\boldsymbol{\varepsilon}\right]\\ &= \boldsymbol{N}+(\boldsymbol{Z}^T)^{-1}\left[\boldsymbol{Z}^T\boldsymbol{T}(\boldsymbol{X}\boldsymbol{\Sigma}^{-1}\boldsymbol{X})^{-1}\boldsymbol{X}^T\boldsymbol{\Sigma}^{-1}\boldsymbol{\varepsilon}\right] \quad (22)\end{aligned}$$

The least-squares baseline estimate for fixed $\check{\boldsymbol{N}}$ is determined from Equation (6), i.e.

$$\boldsymbol{\delta}\hat{\boldsymbol{x}} = (\boldsymbol{G}^T\boldsymbol{\Sigma}^{-1}\boldsymbol{G})^{-1}\boldsymbol{G}^T\boldsymbol{\Sigma}^{-1}(\boldsymbol{y}-\boldsymbol{A}\check{\boldsymbol{N}}), \quad (23)$$

with the baseline error $\boldsymbol{\delta}\hat{\boldsymbol{x}}-\boldsymbol{\delta x}$:

$$\begin{aligned}\boldsymbol{\varepsilon}_{\delta\hat{x}} &= (\boldsymbol{G}^T\boldsymbol{\Sigma}^{-1}\boldsymbol{G})^{-1}\boldsymbol{G}^T\boldsymbol{\Sigma}^{-1}\Big(\boldsymbol{\varepsilon}-\boldsymbol{A}(\boldsymbol{Z}^T)^{-1}\\ &\qquad \left[\boldsymbol{Z}^T\boldsymbol{T}(\boldsymbol{X}^T\boldsymbol{\Sigma}^{-1}\boldsymbol{T})^{-1}\boldsymbol{X}^T\boldsymbol{\Sigma}^{-1}\boldsymbol{\varepsilon}\right]\Big). \quad (24)\end{aligned}$$

The correlated noise vector $\boldsymbol{\varepsilon}$ is factorized by the Choleskey decomposition [11] of the covariance matrix:

$$\boldsymbol{\varepsilon}=\boldsymbol{L}\boldsymbol{s} \quad \text{with} \quad \boldsymbol{\Sigma}=\boldsymbol{L}\boldsymbol{L}^T \quad \text{and} \quad \boldsymbol{s}\sim\mathcal{N}(\boldsymbol{0},\boldsymbol{1}). \quad (25)$$

The baseline error in local coordinates is given by

$$\boldsymbol{\varepsilon}_{\delta\hat{x}} = \boldsymbol{M}_1\boldsymbol{s}-\boldsymbol{M}_2\left[\boldsymbol{M}_3\boldsymbol{s}\right], \quad (26)$$

with the submatrices

$$\begin{aligned}\boldsymbol{M}_1 &= \boldsymbol{R}_\mathrm{L}(\boldsymbol{G}^T\boldsymbol{\Sigma}^{-1}\boldsymbol{G})^{-1}\boldsymbol{G}^T\boldsymbol{\Sigma}^{-1}\boldsymbol{L}\\ \boldsymbol{M}_2 &= \boldsymbol{R}_\mathrm{L}(\boldsymbol{G}^T\boldsymbol{\Sigma}^{-1}\boldsymbol{G})^{-1}\boldsymbol{G}^T\boldsymbol{\Sigma}^{-1}\boldsymbol{A}(\boldsymbol{Z}^T)^{-1}\\ \boldsymbol{M}_3 &= \boldsymbol{Z}^T\boldsymbol{T}(\boldsymbol{X}^T\boldsymbol{\Sigma}^{-1}\boldsymbol{X})^{-1}\boldsymbol{X}^T\boldsymbol{\Sigma}^{-1}\boldsymbol{L}, \quad (27)\end{aligned}$$

and the coordinate transformation matrix $\boldsymbol{R}_\mathbf{L}$. The evaluation of the probability distribution of $\varepsilon_{\delta\hat{x}}$ depends on the probability of rounding $\boldsymbol{M}_3\boldsymbol{s}$ to the k-th non-zero vector $\boldsymbol{\varepsilon}^{(k)}_{\check{\boldsymbol{N}}'}$. The determination of this probability requires the cumulative density function (cdf) of a multivariate gaussian distribution. Unfortunately, no closed form exists for the cdf of a multivariate gaussian distribution.

Importance Sampling (IS) [10] is suggested for probability estimation of rare events. The further analysis restricts to scaling based IS with scaling factor $\sigma_\mathrm{IS}\geq 1$. Traditional IS as described in [10] refers to a scalar random variable. The idea is extended to multi-dimensional IS of correlated random variables and the probability $P\left([\boldsymbol{M}_3\boldsymbol{s}]=\boldsymbol{\varepsilon}^{(k)}_{\check{\boldsymbol{N}}'}\right)$ is approximated by K samples:

$$\hat{P}\left([\boldsymbol{M}_3\boldsymbol{s}]=\boldsymbol{\varepsilon}^{(k)}_{\check{\boldsymbol{N}}'}\right)=\frac{1}{K}\sum_{i=1}^{K}g(\boldsymbol{M}_3\boldsymbol{s}_*^{(i)})\cdot\frac{f(\boldsymbol{M}_3\boldsymbol{s}_*^{(i)})}{f_*(\boldsymbol{M}_3\boldsymbol{s}_*^{(i)})}, \quad (28)$$

with

$$\boldsymbol{s}_*^{(i)}\sim f_*(\boldsymbol{s}_*^{(i)})=\mathcal{N}\left(\boldsymbol{0},\sigma_\mathrm{IS}^2\cdot\boldsymbol{1}^{N_\mathrm{s}-1\times N_\mathrm{s}-1}\right), \quad (29)$$

and

$$\begin{aligned}g(\boldsymbol{M}_3\boldsymbol{s}_*^{(i)}) &= \begin{cases}1 & \text{if} \quad [\boldsymbol{M}_3\boldsymbol{s}_*^{(i)}]=\boldsymbol{\varepsilon}^{(k)}_{\check{\boldsymbol{N}}'}\\ 0 & \text{else.}\end{cases}\\ f(\boldsymbol{M}_3\boldsymbol{s}_*^{(i)}) &= \frac{1}{(2\pi)^{(N_\mathrm{s}-1)/2}|\boldsymbol{M}_3\boldsymbol{M}_3^T|^{1/2}}\\ &\quad\cdot\exp\left(-\frac{1}{2}(\boldsymbol{M}_3\boldsymbol{s}_*^{(i)})^T(\boldsymbol{M}_3\boldsymbol{M}_3^T)^{-1}(\boldsymbol{M}_3\boldsymbol{s}_*^{(i)})\right)\\ f_*(\boldsymbol{M}_3\boldsymbol{s}_*^{(i)}) &= \frac{1}{(2\pi)^{(N_\mathrm{s}-1)/2}|\sigma_\mathrm{IS}^2\boldsymbol{M}_3\boldsymbol{M}_3^T|^{1/2}}\\ &\quad\cdot\exp\left(-\frac{1}{2}(\boldsymbol{M}_3\boldsymbol{s}_*^{(i)})^T(\sigma_\mathrm{IS}^2\boldsymbol{M}_3\boldsymbol{M}_3^T)^{-1}(\boldsymbol{M}_3\boldsymbol{s}_*^{(i)})\right).\end{aligned}$$

Note that there exists only a single scalar weight $w=f(\boldsymbol{M}_3\boldsymbol{s}_*^{(i)})/f_*(\boldsymbol{M}_3\boldsymbol{s}_*^{(i)})$ for each correlated noise vector $\boldsymbol{M}_3\boldsymbol{s}_*^{(i)}$ although the correlation matrix $\boldsymbol{M}_3$ might introduce considerable differences in the variance of the elements of $\boldsymbol{M}_3\boldsymbol{s}_*^{(i)}$. Thus, a trade-off for the common scaling factor σ_IS is required. Both a too small and a too large σ_IS result in few cases where $g(\boldsymbol{M}_3\boldsymbol{s}_*^{(i)})=1$. An estimate of the variance of the IS based probability estimator is derived in [10]. The multi-dimensional generalization is given by

$$\begin{aligned}\hat{\sigma}^2_{P(\varepsilon^{(k)}_{\check{N}'})} &= \frac{1}{K}\left(\frac{1}{K}\sum_{i=1}^{K}\left(g(\boldsymbol{M}_3\boldsymbol{s}_*^{(i)})\cdot\frac{f(\boldsymbol{M}_3\boldsymbol{s}_*^{(i)})}{f_*(\boldsymbol{M}_3\boldsymbol{s}_*^{(i)})}\right)^2\right.\\ &\qquad\left.-\left(\frac{1}{K}\sum_{i=1}^{K}g(\boldsymbol{M}_3\boldsymbol{s}_*^{(i)})\cdot\frac{f(\boldsymbol{M}_3\boldsymbol{s}_*^{(i)})}{f_*(\boldsymbol{M}_3\boldsymbol{s}_*^{(i)})}\right)^2\right) \quad (30)\end{aligned}$$

The k-th integer ambiguity error $\varepsilon^{(k)}_{\check{N}'}$ results in a biased baseline estimate. The bias is obtained from Equation (26):

$$\boldsymbol{\mu}^{(k)}_{\delta\hat{x}} = -\boldsymbol{M}_2\boldsymbol{\varepsilon}^{(k)}_{\check{\boldsymbol{N}}'}. \quad (31)$$

The baseline covariance matrix is conditioned on the fixing error $\varepsilon^{(k)}_{\check{N}'}$. The second term in equation (26) is assumed deterministic so that the conditional covariance matrix is given by

$$\boldsymbol{\Sigma}_{\delta\hat{\boldsymbol{x}}|\left\{[\boldsymbol{M}_3\boldsymbol{s}]=\boldsymbol{\varepsilon}^{(k)}_{\check{\boldsymbol{N}}'}\right\}} = \boldsymbol{R}_\mathrm{L}(\boldsymbol{G}^T\boldsymbol{\Sigma}^{-1}\boldsymbol{G})^{-1}\boldsymbol{R}_\mathrm{L}^T, \quad (32)$$

which is independent of the error vector $\boldsymbol{\varepsilon}^{(k)}_{\check{\boldsymbol{N}}'}$. The pdf of the baseline error is modeled by a weighted superposition of multivariate gaussian distributions:

$$p(\boldsymbol{\varepsilon}_{\delta\hat{\boldsymbol{x}}}) = \sum_{k=1}^{\infty}P\left([\boldsymbol{M}_3\boldsymbol{s}]=\boldsymbol{\varepsilon}^{(k)}_{\check{\boldsymbol{N}}'}\right)\cdot p\left(\boldsymbol{\varepsilon}_{\delta\hat{\boldsymbol{x}}|\left\{[\boldsymbol{M}_3\boldsymbol{s}]=\boldsymbol{\varepsilon}^{(k)}_{\check{\boldsymbol{N}}'}\right\}}\right), \quad (33)$$

with the conditional probability distribution

$$p\left(\varepsilon_{\delta\hat{x}|\left\{[M_3 s]=\varepsilon_{\check{N}'}^{(k)}\right\}}\right) = \frac{1}{2\pi|\Sigma_{\delta\hat{x}|\left\{[M_3 s]=\varepsilon_{\check{N}'}^{(k)}\right\}}|^{1/2}}$$

$$\cdot \exp\left(-\frac{1}{2}(\varepsilon_{\delta\hat{x}} - \mu_{\delta\hat{x}}^{(k)})^T \Sigma^{-1}_{\delta\hat{x}|\left\{[M_3 s]=\varepsilon_{\check{N}'}^{(k)}\right\}} (\varepsilon_{\delta\hat{x}} - \mu_{\delta\hat{x}}^{(k)})\right). \quad (34)$$

Fig. 6 and 7 show the probabilities $\hat{P}_{\mathrm{w}}(\varepsilon_{\check{N}'}^{(k)}) = P\left([M_3 s] = \varepsilon_{\check{N}'}^{(k)}\right)$ of the most likely biases for worst-case geometry. The standard deviations of the probability estimates have been computed with $K = 10^6$ samples and are depicted as a function of σ_{IS}.

The estimated standard deviation $\hat{\sigma}_{\mathrm{P_w}}$ is up to two orders below the estimated probability $\hat{P}_{\mathrm{w}}$. For $\varepsilon_{\check{N}'}^{(k)} = [1, -1, 0, 0, 0]^T$, the optimum scaling factor is $\sigma_{\mathrm{IS}} = 2$ and the uncertainty of P_{w} is reduced by one order of magnitude compared to the Monte Carlo (MC) estimate ($\sigma_{\mathrm{IS}} = 1$). Fig. 7 shows the main benefit of IS as no MC estimate is available for less likely biases. The IS based probability estimation is insensitive w.r.t. σ_{IS}. Small variations in Fig. 7 are caused by a broad range of weights w in Equation (28).

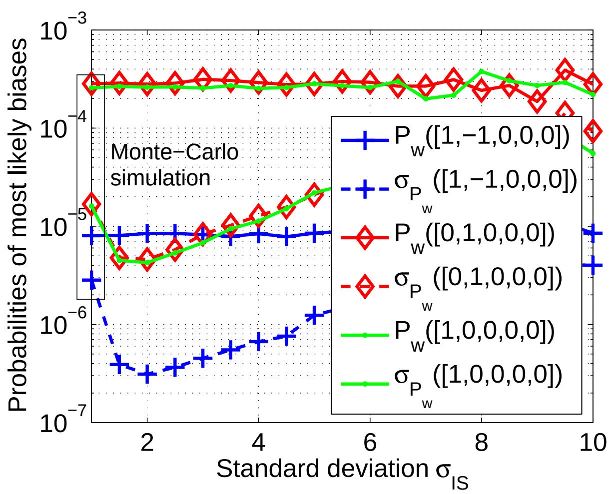

Fig. 6 Probability estimation of most likely SWL biases based on Importance Sampling

PROTECTION LEVEL CONCEPT FOR CARRIER PHASE MEASUREMENTS

The horizontal and vertical protection levels are defined implicitly by the probability distribution of the baseline error in local coordinates:

$$P\left(\sqrt{\varepsilon^2_{\delta\hat{x}}(1,1) + \varepsilon^2_{\delta\hat{x}}(2,2)} > HPL\right) \stackrel{!}{=} 10^{-7} \quad (35)$$

$$P\left(|\varepsilon_{\delta\hat{x}}(3,3)| > VPL\right) \stackrel{!}{=} 10^{-7}. \quad (36)$$

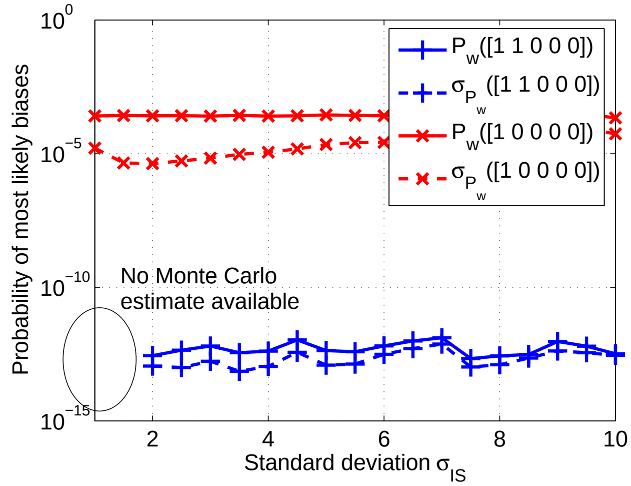

Fig. 7 Probability estimation of most likely SWL biases based on Importance Sampling

Fig. 8 and 9 show the protection levels as a function of time for the first CIR step with a priori SWL knowledge. For simplicity, the correlation between the east and north component of the baseline error estimate has been neglected. The VPL exceeds the HPL with a maximum of $1.05\mathrm{m}$.

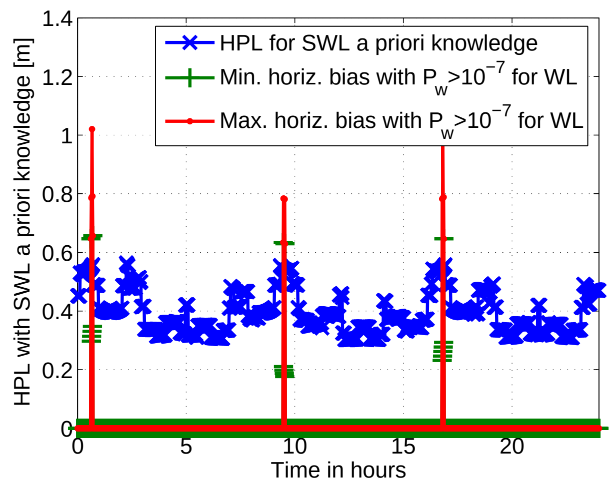

Fig. 8 HPL with SWL a priori knowledge and its benefit for the detection of WL biases

BIAS DETECTION WITH CASCADE AMBIGUITY RESOLUTION

The horizontal and vertical baseline errors exceed the SWL protection levels with a probability of 10^{-7}. The SWL measurements might also be used for bias detection during the WL fixing. The WL biases must fulfill two criterions to be excluded: The biases must be larger than the SWL protection level and occur with a probability larger

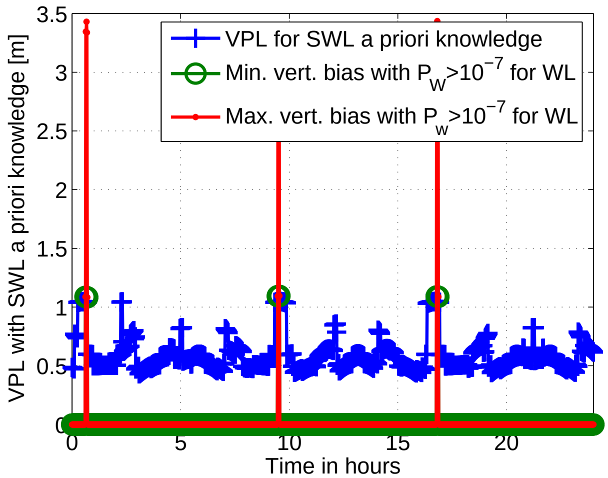

Fig. 9 VPL with SWL a priori knowledge and its benefit for the detection of WL biases

than 10^{-7}. Fig. 8 shows minimum and maximum horizontal WL biases with a probability of at least 10^{-7}. The lower and upper limits of vertical WL biases are depicted in Fig. 9. All WL biases can be excluded because the minimum vertical WL bias is always larger than the SWL VPL.

CONCLUSIONS

In this paper, the LAMBDA algorithm is applied to each step of Cascade Integer Resolution (CIR). The widelane combination has been optimized such that the probability of wrong integer fixing is minimized. The probability distribution of the baseline error including error prone ambiguity fixing is estimated using a mixed multi-variate probability distribution. Decorrelation transformations, search processes as well as rounding operations are taken into account. The baseline biases due to error-prone integer fixing are analysed by importance sampling. A protection level concept for differential carrier phase measurements is presented and used for bias detection in CIR.

Future work might concentrate on the development of carrier phase based Receiver Autonomous Integrity Monitoring (RAIM) and the exclusion of faulty satellites. In the tracking mode analysis, the integer estimate of each satellite is easily verified with the a priori knowledge of all other integer ambiguities.

REFERENCES

[1] B. Forssell, M. Martin-Neira and R. Harris, *Carrier Phase Ambiguity Resolution in GNSS-2*, Proceedings of the Institute of Navigation (ION GPS), Kansas City, 1997

[2] P.J.G. Teunissen, *Least-squares estimation of the integer ambiguities*, Invited lecture, Section IV, Theory and Methodology, IAG General Meeting, Beijing, China, 1993.

[3] P.J.G. Teunissen and A. Kleusberg, *GPS for Geodesy*, Springer, 2nd edition, Jan. 1998.

[4] P. de Jonge and C. Tiberius, *The LAMBDA method for integer ambiguity estimation: implementation aspects*, Publications of the Delft Geodetic Computing Centre, no. 12, Aug. 1996.

[5] J. Jung, P. Enge, and B. Pervan, *Optimization of Cascade Integer Ambiguity Resolution with Three Civil GPS Frequencies*, Proc. of the Institute of Navigation (ION), 2000.

[6] P. Collins, *An overview of GPS inter-frequency carrier phase combinations*, 1999.

[7] W. Zhang, *Triple frequency Cascading Ambiguity Resolution for Modernized GPS and Galileo*, UCGE Reports, No. 20228, 2005.

[8] K. Koch, *Parameter Estimation and Hypothesis Testing in Linear Models*, 2nd edition, Springer, 1999.

[9] S. Verhagen, *On the Reliability of Integer Ambiguity Resolution*, Journal of the Institute of Navigation, Vol. 52, No. 2, pp. 99-110, 2005.

[10] R. Srinivasan, *Importance Sampling: Applications in Communications and Detection*, Springer, 2002.

[11] G. Golub and C. Loan, *Matrix Computations*, Johns Hopkins University Press, Baltimore, MD, 2nd edition, 1989.